Received: 9 August 2021 | Revised: 21 September 2021 | Accepted: 27 September 2021

DOI: 10.1111/cas.15156

ORIGINAL ARTICLE

Cancer Science WILEY

Prediction of the effects of radiation therapy in esophageal cancer using diffusion and perfusion MRI

Peiliang Wang[1] | Xin Wang[2] | Liang Xu[3] | Jinming Yu[1,2] | Feifei Teng[2]

[1]Department of Radiation Oncology, Shandong Cancer Hospital and Institute, Cheeloo college of medicine, Shandong University, Jinan, China

[2]Department of Radiation Oncology, Shandong Cancer Hospital and Institute, Shandong First Medical University and Shandong Academy of Medical Sciences, Jinan, China

[3]Department of Radiology, Shandong Cancer Hospital and Institute, Shandong First Medical University and Shandong Academy of Medical Sciences, Jinan, China

Correspondence
Feifei Teng, Department of Radiation Oncology, Department of Radiation Oncology, Shandong Cancer Hospital and Institute, Shandong First Medical University and Shandong Academy of Medical Sciences, Jinan, China.
Email: tengfeifei16@126.com

Funding information
National Natural Science Foundation of China, Grant/Award Number: NSFC81803066; Shandong Provincial Natural Science Foundation, Grant/Award Number: ZR2019BH046

Abstract

Chemoradiation therapy (CRT) of locally advanced esophageal cancer (LAEC), although improving outcomes of patients, still results in 50% of local failure. An early prediction could identify patients at high risk of poor response for individualized adaptive treatment. We aimed to investigate physiological changes in LAEC using diffusion and perfusion magnetic resonance imaging (MRI) for early prediction of treatment response. In the study, 115 LAEC patients treated with CRT were enrolled (67 in the discovery cohort and 48 in the validation cohort). MRI scans were performed before radiotherapy (pre-RT) and at week 3 during RT (mid-RT). Gross tumor volume (GTV) of primary tumor was delineated on T2-weighted images. Within the GTV, the hypercellularity volume (V_{HC}) and high blood volume (V_{HBV}) were defined based on the analysis of ADC and fractional plasma volume (Vp) histogram distributions within the tumors in the discovery cohort. The median GTVs were 28 cc ± 2.2 cc at pre-RT and 16.7 cc ± 1.5 cc at mid-RT. Respectively, V_{HC} and V_{HBV} decreased from 4.7 cc ± 0.7 cc and 5.7 cc ± 0.7 cc at pre-RT to 2.8 cc ± 0.4 cc and 3.5 cc ± 0.5 cc at mid-RT. Smaller V_{HC} at mid-RT (area under the curve [AUC] = 0.67, $P = .05$; AUC = 0.66, $P = .05$) and further decrease in V_{HC} at mid-RT (AUC = 0.7, $P = .01$; AUC = 0.69, $P = .03$) were associated with longer progression-free survival (PFS) in both discovery and validation cohort. No significant predictive effects were shown in GTV and V_{HBV} at any time point. In conclusion, we demonstrated that V_{HC} represents aggressive subvolumes in LAEC. Further analysis will be carried out to confirm the correlations between the changes in image-phenotype subvolumes and local failure to determine the radiation-resistant tumor subvolumes, which may be useful for dose escalation.

KEYWORDS
diffusion, locally advanced esophageal cancer, magnetic resonance imaging, perfusion, radiation therapy

Peiliang Wang and Xin Wang contributed equally to this work.

1 | INTRODUCTION

Concurrent chemoradiotherapy (CRT) has been the standard therapy for patients with inoperable locally advanced esophageal cancer (LAEC). Although significantly improving in local/regional control and overall survival (OS), it still results in local failure in 50% of cases.[1-3] Higher radiation dose has been explored as a potential improvement.[4-7] However, the results were controversial with higher treatment toxicity and limited survival benefit. Therefore, an early prediction of treatment outcome during therapy using noninvasive imaging could identify the patients at high risk for failure for individualized adaptive treatment.

2-deoxy-2-[fluorine-18] fluoro-D-glucose positron emission tomography/computed tomography (^{18}F-FDG PET/CT) has been employed for predicting early responses to CRT for esophageal cancer (EC) patients by using the metabolic parameters including metabolic tumor volume (MTV) and the maximum of standard uptake value (SUVmax). Besides, total lesion glycolysis (TLG) was suggested to be more reliable to predict the treatment response to neoadjuvant therapy in a smaller number of patients, reflecting both mean metabolic FDG uptake and tumor volume.[8-11] However, this method has not yet been established in routine clinical practice.[12,13]

Presently, the role of magnetic resonance imaging (MRI) has been investigated for prediction of treatment failure in EC.[14,15] Diffusion-weighted (DW) imaging, a quantitative measure of water motion in tissue and sensitive to cellularity, has shown that an increase in apparent diffusion coefficient (ADC) of the EC during neoadjuvant CRT (nCRT) is associated with positive therapy response.[16,17] Additionally, dynamic contrast–enhanced (DCE)-MRI assesses relative tumor blood volume (BV) and vascular permeability, which are associated with neoangiogenesis and tumor growth.[18,19] Poorly perfused and highly hypoxic tumors all have been correlated with worse outcomes in EC.[20] The predictive effects of perfusion MRI in LAEC are largely unknown.

Heterogenicity in EC has been recognized.[20,21] Also, RT effects on high and low diffusion and perfusion regions may be different. All these indicate that an analysis of the maximum, median, or mean imaging parameters within the whole tumor volume may be inadequate. Because hypercellularity and poor perfusion reflect subvolumes with distinct biologic characteristics associated with treatment resistance, we hypothesized that these subvolumes defined by functional MRI could be useful to predict the response to CRT in LAEC. Therefore, we investigated the physiological changes in LAECs during the course of CRT using diffusion and perfusion MRI for early prediction of treatment response and correlated the changes in image-phenotype subvolumes with local failure to determine the radiation-resistant tumor subvolumes, which may be useful for dose escalation.

2 | MATERIALS AND METHODS

2.1 | Patient population and treatment

As shown in Figure 1 and Figure S1, 115 consecutive patients with inoperable LAEC were enrolled in an institutional review board–approved study and signed informed consents. Patients were allocated to discovery and validation cohorts according to the time of radiotherapy in a 1:1 ratio; the first 67 patients were allocated to the discovery cohort, and the subsequent 48 were allocated to the validation cohort. All patients received definite thoracic radiotherapy (RT) and concurrent chemotherapy. RT was delivered with intensity-modulated RT with a median dose of 50 Gy in 25 fx to the primary tumor and involved lymph nodes positive on CT or PET and a boost to the primary tumor for a total of 60 Gy (range from 58 to 64 Gy). Chemotherapy was administered concurrently with RT to all patients consisting of 5-fluorouracil with either platinum- or taxane-based regimen.

2.2 | MRI scans

Patients underwent MRI scanning at two time points: within 1 week before RT (pre-RT) and during RT at a median of 3 weeks (range from 2.4 to 3.3 weeks) after initiation of RT (mid-RT). All MRI scans were performed on a 3T scanner (Skyra, Siemens), including post-contrast T1-weighted images, T1-weighted dynamic contrast–enhanced (DCE) images, T2-weighted images, and diffusion-weighted images (DWI). Detailed image acquisition parameters are presented in Doc. S1.

2.3 | Image analysis and registration

BV maps were quantified from T1-weighted DCE-MRI using the modified Tofts model implemented in an in-house analysis tool.[21] The ADC maps were derived from DWI with b-values of 0 and 800 s/mm^2 by in-house software. DWI were coregistered to post-contrast T1-weighted images for each patient using rigid body transformation. The post-contrast T1-weighted images were used as target for registration of BV and ADC maps.

2.4 | Tumor volumes and subvolumes

Gross tumor volume (GTV) of primary tumor was delineated based on T2-weighted images by three radiation oncologists with a median of 5 years of experience in interpreting MRI scans and estimating GTV. Inter- and intraobserver reproducibility of GTV delineation were initially analyzed with the GTV data of 30 randomly selected patients. To ensure reproducibility, each oncologist repeated delineating the GTVs twice with an interval of at least 2 weeks, following the same procedure. Intraclass correlation coefficients (ICCs) were used for evaluating the intra- and inter-observer agreement in terms of GTV delineation. We interpreted an ICC of 0.81-1.00 as almost perfect agreement, 0.61-0.80 as substantial agreement, 0.41-0.60 as moderate agreement, 0.21-0.40 as fair agreement, and 0-0.20 as poor or no agreement.[22] An ICC greater than 0.6 was considered a mark of satisfactory

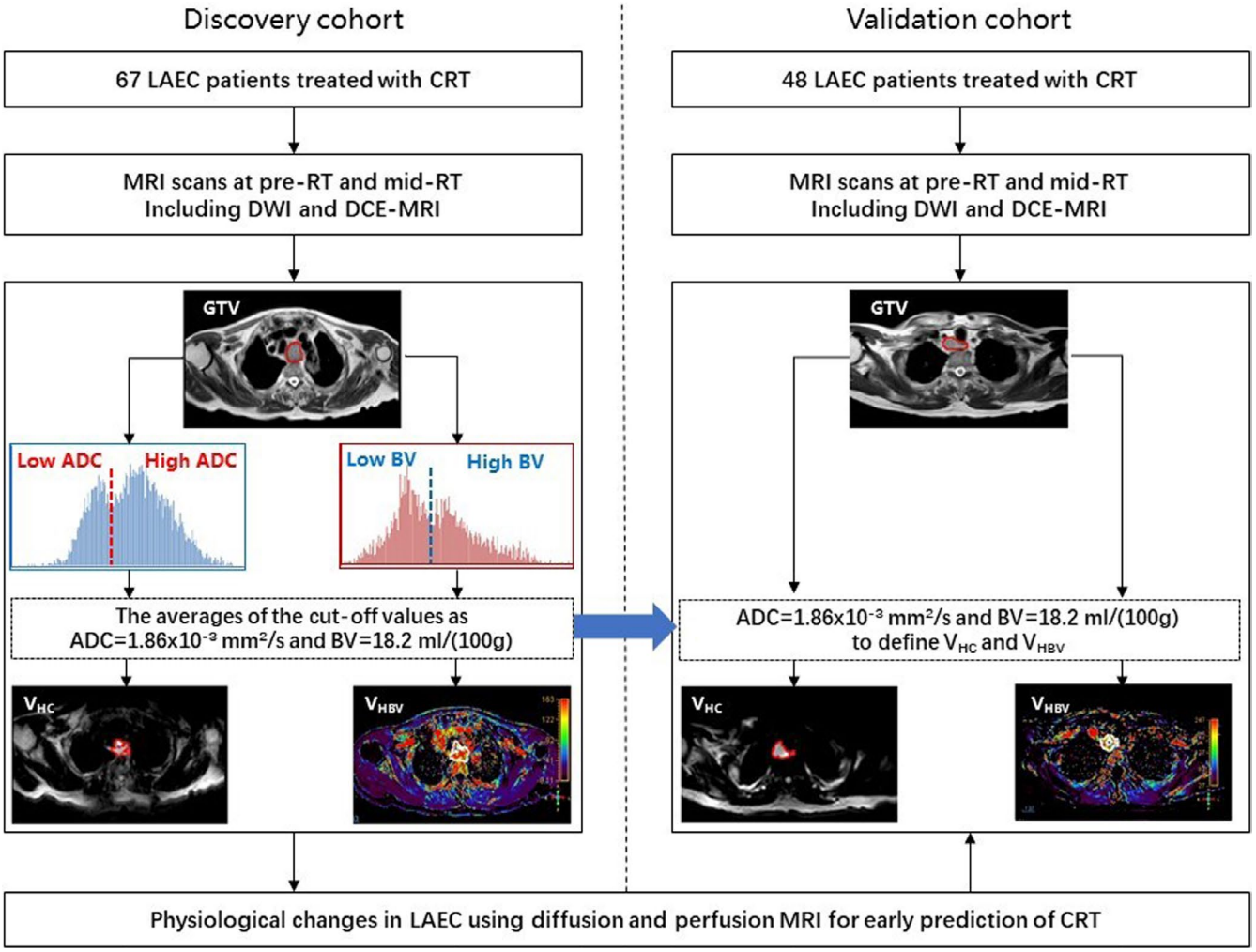

FIGURE 1 Patient recruitment and study design. In total, 115 locally advanced esophageal cancer (LAEC) patients with pre-RT and mid-RT multiparametric magnetic resonance imaging (MRI) were enrolled in this study. ADC, apparent diffusion coefficient; BV, blood volume; CRT, chemoradiotherapy; DCE, dynamic contrast-enhanced; DWI, diffusion-weighted images; RT, radiotherapy; V_{HBV}, high BV volume; V_{HC}, hypercellularity subvolume

intra- and interobserver reproducibility. To ensure the accuracy of tumor masking, the GTV delineations were evaluated following the same guideline by another radiologist with 6 years of estimating GTV.

A hypercellularity subvolume (V_{HC}) of the primary tumor was defined as ADC $< 1.86 \times 10^{-3}$ mm^2/s within the GTV, and high blood volume (V_{HBV}) was defined using the threshold of BV > 18.2 ml/100 g within the GTV. The threshold of BV and ADC were defined based on the analysis of fractional plasma volume (Vp) and ADC histogram distributions within the tumors in the discovery cohort. The lumen of esophagus, whose ADC values and BV values exceeded the thresholds, was excluded automatically from the subvolumes of V_{HC} and V_{HBV}. Afterward, we checked again and manually removed the obvious blood vessels and cavities within the subvolumes to reduce their influence on the results. Representative images are shown in Figure 2.

The subvolumes in lymph nodes were not investigated in this analysis because of the limited spatial coverage by diffusion imaging.

2.5 | Follow-up

After treatment, the patients were followed up with physician visits, CT or PET/CT scans, and laboratory examinations every 2-3 months. The date of progression was defined according to the clinical and radiographic criteria as determined by the multidisciplinary team in the course of clinical care as documented in the medical records. Progression and regression were assessed by both gastrointestinal oncologists and radiation oncologists according to RECIST criteria. Progression-free survival (PFS) was defined as the interval from the date of diagnosis to the date of local progression, death, or last follow-up. OS was defined as the interval from the date of diagnosis to death from any cause or last follow-up.

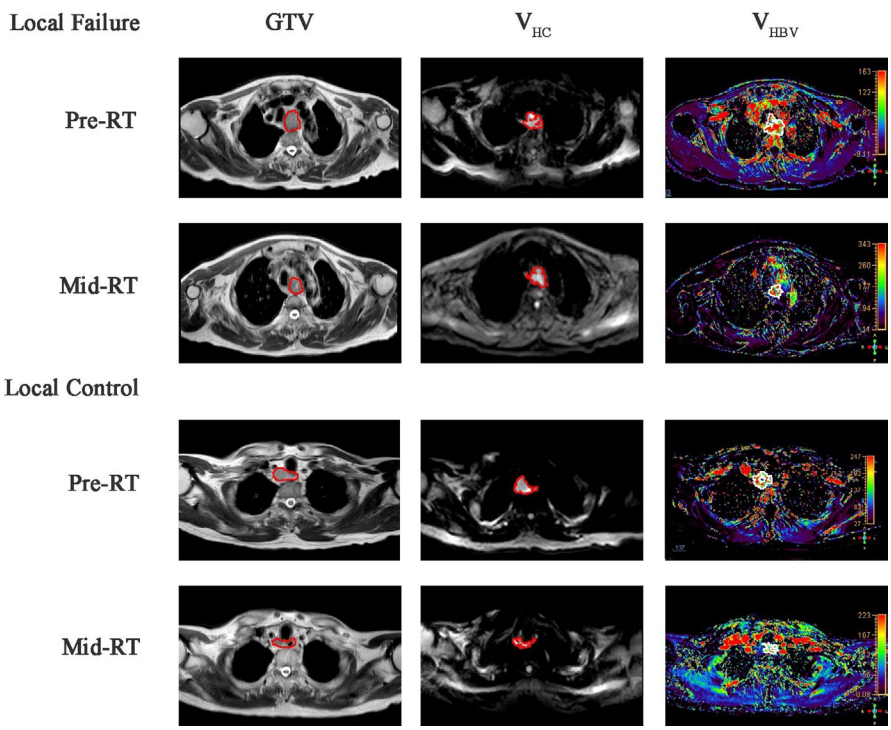

FIGURE 2 Representative images of two patients with local failure and local control. Gross tumor volume (GTV) of primary disease was delineated based on T2-weighted images (left). A hypercellularity subvolume (V_{HC}) of the primary tumor was defined as apparent diffusion coefficient (ADC) $<1.86 \times 10^{-3}$ mm^2/s within the gross tumor volume (GTV) (second left), and the high BV volume (V_{HBV}) by using the threshold of blood volume (BV) >18.2 ml/(100 g) within the GTV (second right). Patients with larger V_{HC} at mid-RT had a worse prognosis and showed recurrence within V_{HC} at mid-RT. RT, radiotherapy

2.6 | Data and statistical analysis

Descriptive statistics were summarized as mean ± SD. The relative changes of the subvolumes were compared between pre-RT and mid-RT using the Mann-Whitney U test or *t*-test for quantitative variables and with the chi-square test or Fisher's test for qualitative variables. The area under the curve (AUC) of the receiver operating characteristic (ROC) curve was calculated to assess the prediction abilities of the imaging metrics for CRT outcomes. Associations of the imaging metrics pre-RT and mid-RT and their changes during RT with PFS and OS of patients were analyzed by Cox proportional hazards regression analysis. All statistical analyses were two sided and *P*-values less than .05 indicating statistical significance. The statistical analyses were performed using SPSS software, version 21 (SPSS).

3 | RESULTS

3.1 | Associations of patient characteristics with tumor pre-RT subvolumes

Between January 2016 and January 2020, a total of 115 consecutive patients with newly diagnosed LAEC who underwent standard diagnostic work-up signed informed consent. Characteristics of patients are listed in Table 1 and Table S1. Histologic tumor types were squamous cell carcinoma (SCC) for all patients. There were no significant differences in clinical characteristics between the discovery and validation cohorts (Table S1). Also, no significant associations were observed in age, gender, Karnofsky Performance Status (KPS) score, clinical T stage, and tumor location with tumor pre-RT subvolumes in the discovery and validation cohorts (Table 1).

3.2 | Changes of GTV and image-phenotype subvolumes during RT

Satisfactory inter- and intraobserver reproducibility of GTV delineating was achieved with ICC >0.6 both among the GTVs delineated by the three oncologists at baseline and among the GTVs from the same oncologist at baseline and at least 2 weeks later.

For patients in the discovery cohort, the median pre-RT GTV was 28 cc ± 3.2 cc, with a decrease of −32.5% ± 7.2% to 16.5 cc ± 2.2 cc at mid-RT. Respectively, V_{HC} and V_{HBV} decreased from 5.6 cc ± 1.1 cc and 4.5 cc ± 1.1 cc at pre-RT to 4.1 cc ± 0.7 cc and 3.2 cc ± 0.7 cc at mid-RT. For patients in the validation cohort, the pre- to mid-RT GTV shrinkage was 41.1%, from 25.7 cc ± 2.6 cc to 17.0 cc ± 2.1 cc, and V_{HC} and V_{HBV} shrank from 8.7 cc ± 1.0 cc and 6.5 cc ± 0.6 cc to 5.6 cc ± 0.6 cc and 4.4 cc ± 0.5 cc, respectively. There were no significant differences in the image-phenotype subvolumes between the discovery and validation cohorts (Table S1).

3.3 | Clinical outcomes

With a median follow-up period of 35.5 months, the median PFS was 13.5 months for the discovery cohort and 13.1 months for the validation cohort. The median OS was 18.0 months for the discovery cohort and 18.4 months for the validation cohort. As shown in Table 2, mid-RT V_{HC} and pre- to mid-RT V_{HC} shrinkage showed good prediction performance for PFS with AUCs of 0.67 ($P = .05$) and 0.7 ($P = .01$) for patients in the discovery cohort. The prognostic effects of mid-RT V_{HC} and early changes of V_{HC} during RT were also observed in the validation cohort with AUCs of 0.66 ($P = .05$) and 0.69 ($P = .03$) (Table 2). In univariate analysis, smaller V_{HC} at mid-RT

TABLE 1 Associations of patient characteristics with tumor pre-RT subvolumes

	Discovery cohort						Validation cohort					
	GTV pre-RT	*P*-value	V_{HC} pre-RT	*P* value	V_{HBV} pre-RT	*P* value	GTV pre-RT	*P*-value	V_{HC} pre-RT	*P*-value	V_{HBV} pre-RT	*P*-value
Age (years)												
<60	30.5 ± 4.6	.74	6.7 ± 2.5	.52	5.1 ± 1.5	.12	25.7 ± 3.8	0.64	4.0 ± 1.1	.71	6.5 ± 0.9	.15
>60	25.8 ± 4.2		4.6 ± 1.1		4.5 ± 1.4		30.3 ± 3.3		4.6 ± 0.6		7.0 ± 0.8	
Gender												
Male	24.6 ± 3.8	.59	6.5 ± 1.2	.94	4.5 ± 1.3	.94	30.3 ± 3.0	.62	3.8 ± 1.3	0.31	6.2 ± 0.8	.58
Female	40.1 ± 5.7		3.8 ± 2.5		6.7 ± 2.3		24.4 ± 4.6		4.5 ± 0.6		7.2 ± 1.2	
KPS score												
<80	27.9 ± 6.5	.48	6.1 ± 2.1	.45	4.1 ± 2.1	.79	36.6 ± 4.2	.59	4.4 ± 1.0	0.25	6.5 ± 1.3	.72
>80	28.0 ± 3.5		5.6 ± 1.2		4.5 ± 1.2		25.7 ± 3.1		4.3 ± 0.7		6.5 ± 0.7	
Clinical T stage												
2	26.3 ± 8.5	.89	6.9 ± 3.2	.18	6.1 ± 1.9	.21	32.3 ± 6.8	.07	6.1 ± 2.9	0.15	8.0 ± 1.4	.08
3	30.2 ± 4.3		5.6 ± 1.3		4.5 ± 1.7		23.8 ± 3.1		3.9 ± 0.8		6.5 ± 0.6	
4	27.1 ± 5.7		6.0 ± 2.2		4.4 ± 1.6		36.6 ± 4.6		5.2 ± 0.7		6.5 ± 1.3	
Tumor location												
Proximal esophagus	21.1 ± 7.5	.82	4.5 ± 3.3	.71	6.2 ± 2.3	.75	23.7 ± 6.8	.95	3.8 ± 0.6	.43	5.9 ± 1.9	.46
Middle esophagus	30.2 ± 4.2		3.7 ± 1.2		4.0 ± 1.7		25.7 ± 3.9		4.8 ± 1.0		6.2 ± 0.6	
Distal esophagus	29.3 ± 6.4		6.2 ± 1.7		4.5 ± 1.9		36.5 ± 4.1		4.0 ± 0.7		8.1 ± 0.9	
Gastroesophageal junction	27.8 ± 13.5		5.8 ± 5.6		3.4 ± 4.7		37.6 ± 7.6		5.3 ± 2.3		6.5 ± 3.2	

TABLE 2 AUC of image-phenotype subvolumes in discovery and validation cohorts

	Discovery cohort			Validation cohort		
	Cutoff	AUC	*P*-values	Cutoff	AUC	*P*-values
GTV pre-RT	33.1 cc	0.53	.67	19.0 cc	0.53	.74
GTV mid-RT	13.3 cc	0.50	.97	19.0 cc	0.61	.22
ΔGTV	-54%	0.52	.78	-10.4%	0.61	.18
V_{HC} pre-RT	7.3 cc	0.51	.89	5.2 cc	0.52	.82
V_{HC} mid-RT	1.1 cc	0.67	.05	2.5 cc	0.66	.05
ΔV_{HC}	-63%	0.70	.01	-35%	0.69	.03
V_{HBV} pre-RT	10.4 cc	0.52	.87	7.5 cc	0.57	.42
V_{HBV} mid-RT	3.3 cc	0.54	.63	5.5 cc	0.60	.25
ΔVHBV	-54%	0.58	.27	-44.5%	0.65	.07

and more shrinkage in V_{HC} at mid-RT were associated with longer PFS and OS (Table 3). Kaplan-Meier curves of PFS and OS according to V_{HC} at mid-RT and the shrinkage in V_{HC} at mid-RT are shown in Figure 3. In addition, patients with better clinical stage showed more favorable PFS and OS in both the discovery and validation cohort. No significant predictive effects were shown in GTV, V_{HBV}, and other clinical characteristics.

4 | DISCUSSION

The present study was designed to investigate the physiological changes in LAECs during the course of CRT using diffusion and perfusion MRI for early prediction of treatment response. We found that large V_{HC} delineated on DWI at 3 weeks after initiation RT and increasing volumes in V_{HC} during RT was associated with a worse prognosis. It indicated that tumor subvolumes containing hypercellularity represented radiation-resistant tumor subvolumes, which may benefit from treatment intensification.

Concurrent CRT has been the standard therapy for inoperable LAEC; although improving outcomes of patients, it still results in local failure in 50% of cases. In an attempt to improve local control, escalation in radiation dose has been tried in several trials.[4,6] In the INT 0123 trial, the higher radiation dose did not increase survival or local/regional control. In a phase 1/2 trial conducted by Welsh et al.,[6] the radiotherapy plan was 50.4 Gy to subclinical areas at risk and 63 Gy to the gross tumor and involved nodes. Of patients with relatively large boosted volumes, 22% developed acute grade 3 toxic events such as esophagitis, dysphagia, and anorexia, and 7% developed late grade 3 toxic events such as esophageal strictures. Higher radiation dose has been deemed to be needed for SCC and often resulted in higher treatment toxicity and limited survival benefit with large target volumes.[23] Therefore, determining the radiation-resistant subvolumes is much more important in patients with SCC to guide dose-escalated radiation. This study provided an encouraging result for the potential value of MRI in predicting treatment response to CRT, predicting sites of local recurrence, and guiding dose-escalated radiation for patients with LAEC.

Some previous studies showed that sequential ^{18}F-FDG PET/CT during treatment can be used to predict outcomes after radiotherapy and chemotherapy for EC.[24] SUVmax, MTV, and TLG have been approved as valuable metabolic parameters to predict tumor response in PET/CT.[25] A prospective multicenter study evaluated the combined value of ^{18}F-FDG PET/CT and DW-MRI during and after nCRT to predict pathologic response in patients who undergo nCRT for EC. It was found that a multimodality imaging approach, instead of a single modality, may provide complementary value for predicting pathologic response.[15] Previous studies have shown that ^{18}F-FDG PET/CT and MRI are both well-tolerated imaging procedures for evaluating the response to treatment of EC.[26] Also, most previous studies demonstrated the predictive effects of ^{18}F-FDG PET/CT on the assessment of pathologic complete response instead of long-term treatment outcomes, which may outweigh short-term attributes.[27] As ^{18}F-FDG PET/CT scanning before and during CRT are currently not included in standard imaging evaluation, the predictive value should be considered in light of the associated costs and physical burden to the patients of repeated imaging scans. In our study, only eight patients in the discovery cohort and 12 patients in the validation cohort underwent PET/CT scan, so we failed to analyze that imaging information. Further study will be carried out to analyze the relationships bewteen the changes in ^{18}F-FDG PET/CT and those in DW-MRI and the predictive effect of the combined multimodality imaging approach during CRT for LAEC.

Until now, most MR imaging studies in EC treatment response prediction have focused on the mean, median, or maximum imaging parameters within the whole tumor volume or region of interest (ROI).[15-17] A pilot study explored the value of DW-MRI for the prediction of pathological response to nCRT in EC.[16] The median ADC value of the whole tumor volume was used in that study. It was found that the change in ADC during the first 2-3 weeks of nCRT for EC seemed highly predictive of pathologic response. These results were also validated in another pilot study.[17] Besides the tumor volume ADC mean value, the 25th and 10th percentiles were found associated with pathologic response. Recently, a prospective multicenter study with a larger cohort of 82 EC patients evaluated the combined value of ^{18}F-FDG PET/CT and DW-MRI

TABLE 3 Univariable analysis of PFS and OS

	Discovery cohort						Validation cohort					
	PFS			OS			PFS			OS		
	HR	95% CI	*P*-value	HR	95% CI	*P*-value	HR	95% CI	*P*-value	HR	95%CI	*P* value
Age	1.16	0.60-2.25	.67	1.26	0.61-2.60	.53	1.01	0.49-2.07	.98	1.13	0.55-2.33	.74
Gender	2.00	0.84-4.76	.12	2.01	0.79-5.24	.14	0.91	0.41-2.04	.82	1.46	0.59-3.59	.41
KPS	1.46	0.72-2.96	.30	1.40	0.64-3.07	.40	1.17	0.64-2.28	.65	0.76	0.37-1.56	.46
T stage	1.12	0.75-2.91	.40	1.06	0.57-1.87	.52	1.15	0.65-2.03	.62	1.13	0.64-1.99	.68
Clinical stage	1.31	1.07-1.63	.02*	1.23	0.98-1.54	.06	1.63	1.23-2.19	.01*	1.55	1.07-2.23	.02*
Tumor sites	0.81	0.56-1.17	.26	0.87	0.58-1.29	.49	1.43	0.96-2.14	.08	1.29	0.85-1.96	.23
GTV pre-RT	1.59	0.88-2.88	.13	1.12	0.59-2.13	.73	1.28	0.64-2.62	.17	0.99	0.40-2.44	.98
GTV mid-RT	1.06	0.63-1.74	.89	0.83	0.44-1.57	.57	1.49	0.73-3.06	.28	1.55	0.76-3.18	.23
ΔGTV	1.09	0.55-2.16	.80	0.93	0.46-1.88	.83	1.08	0.37-3.14	.89	0.79	0.24-2.64	.71
V_{HC} pre-RT	1.47	0.81-2.68	.21	1.26	0.65-2.41	.49	1.26	0.62-2.56	.52	1.77	0.54-2.33	.77
V_{HC} mid-RT	2.28	1.10-4.77	.03*	2.36	1.04-5.38	.04*	1.97	1.00-3.99	.05*	2.60	1.24-5.46	.01*
ΔV_{HC}	1.95	0.99-3.82	.05*	2.34	1.10-4.99	.03*	2.16	1.01-4.59	.04*	3.02	1.33-6.80	.01*
V_{HBV} pre-RT	1.47	0.94-2.74	.14	1.01	0.68-2.03	.86	0.67	0.32-1.41	.29	0.64	0.30-1.33	.23
V_{HBV} mid-RT	1.29	0.71-2.34	.39	1.25	0.66-2.36	.49	0.97	0.46-2.08	.94	1.01	0.51-2.23	.87
ΔV_{HBV}	1.45	0.75-2.79	.27	1.54	0.77-3.08	.22	0.88	0.42-1.84	.73	1.18	0.57-2.49	.65

HR, Hazard Ratio; CI, Confidence Interval; *Statistically significant.

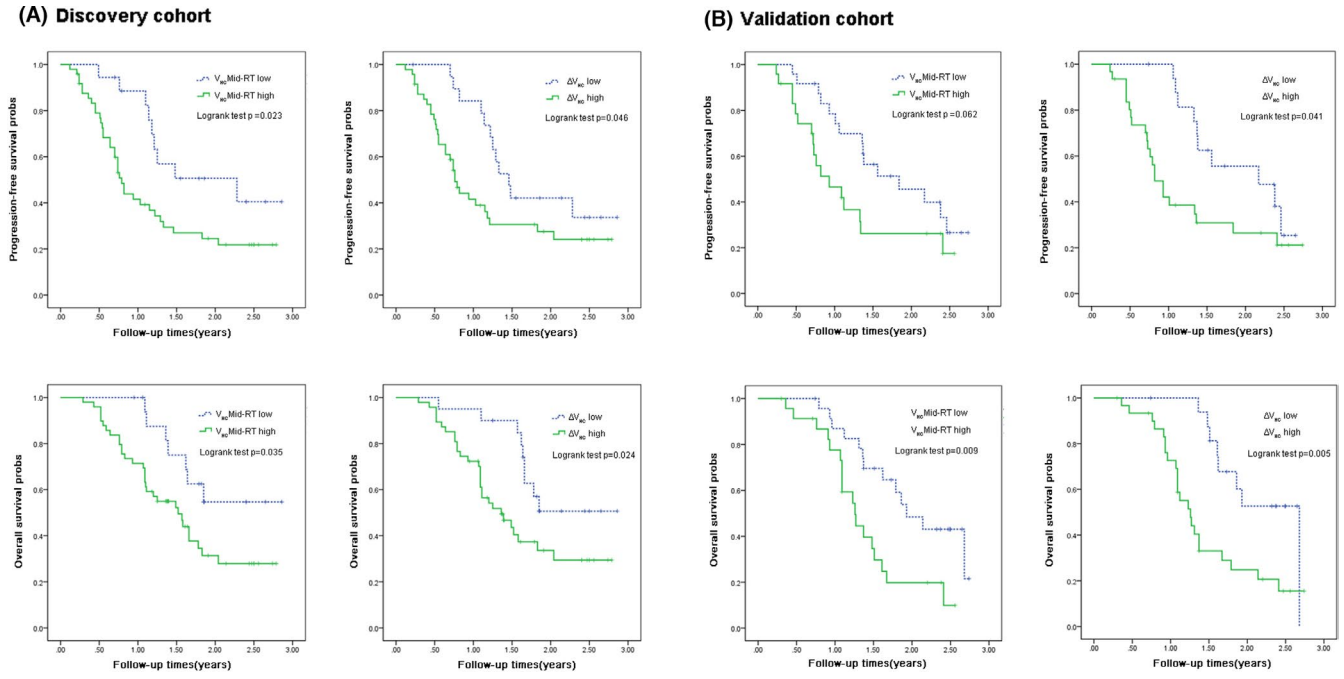

FIGURE 3 Progression-free survival and overall survival according to hypercellularity subvolume (V_{HC}) at mid-RT and the shrinkage in V_{HC} at mid-RT (ΔV_{HC}) in the discovery cohort (A) and validation cohort (B). RT, radiotherapy

during and after nCRT to predict pathologic response.[15] All of the above studies suggested the predictive value of DW-MRI, which was consistent with our results. However, the imaging parameters used by those previous studies neglected tumor heterogenicity, which has been proved pivotal in tumor progression and response to treatment. Therefore, we analyzed tumor subvolumes of low ADC and high BV instead of the mean values of these imaging parameters.

The thresholds of BV and ADC were defined based upon the analysis of Vp and ADC histogram distributions within the tumors in the discovery cohort. Thresholds were used for determining the subvolumes of HBV and low ADC; we used the threshold values reported in the literature and compared them with our own data. Nevertheless, we performed voxel-level correlations that were independent of thresholds used and showed similar results.

Tumor perfusion situation has variable effects on treatment response and prognosis in different tumor types. Poorly perfused and highly hypoxic tumors have been correlated with worse outcomes in head and neck squamous cell cancer (HNSCC).[28,29] Persisting poorly perfused tumor subvolumes during the course of radiotherapy have been demonstrated associated with high risk of local failure, and perfusion MRI and hypoxic PET have been used for boosting target definition in HNSCC. However, elevated cerebral blood volume (CBV) was an adverse prognostic factor in glioblastoma and was associated with worse treatment response.[18,19,30,31] Tumor hypoxia has been confirmed in EC, but the prognostic value was not consistent across previous studies.[32] This might arise from different methodology for hypoxia detection and quantification. PET-based hypoxia imaging has shown potential in evaluating tumor hypoxic status,[33,34] but DCE-MRI has not been widely used for evaluating the outcomes in EC. In our results, V_{HBV} was not found associated with outcomes of patients. In further studies, the combination of multiple imaging markers might be a potential tool to evaluate the hypoxic status and individualized hypoxia-adaptive treatment to improve radiotherapy response in EC patients.

4.1 | Limitations

There are some limitations of the current study. First, though the sample size was relatively large, an external validation cohort from another institution was absent to validate our results. Second, the geometric distortion of ADC maps and the target displacement errors between ADC maps and T2-weighted images need to be quantified and reduced in future analysis of patterns of failure.

5 | CONCLUSIONS

In conclusion, our study shows that large hypercellularity volumes delineated on DWI during RT and increasing volumes in V_{HC} during RT were associated with a worse prognosis. It indicated that tumor subvolumes containing hypercellularity represented radiation-resistant tumor subvolumes, which may benefit from treatment intensification. Additional larger prospective studies and other combined multimodal imaging approaches are needed to validate these results.

6 | ETHICAL CONSIDERATIONS

The methods and procedures for this study were approved by the Research Ethics Board of Shandong Cancer Hospital and have followed the principles outlined in the Declaration of Helsinki for all human investigations. Individual consent was waived owing to its retrospective nature.

ACKNOWLEDGEMENTS

This work was supported by grants from the National Natural Science Foundation of China (NSFC81803066) and the Shandong Provincial Natural Science Foundation (ZR2019BH046) to FFT.

CONFLICT OF INTEREST

The authors have no conflict of interest.

DATA AVAILABILITY STATEMENT

The data used and analyzed in this study are available from the corresponding author on reasonable request.

ORCID

Peiliang Wang https://orcid.org/0000-0001-7479-0277
Feifei Teng https://orcid.org/0000-0001-8101-9405

REFERENCES

1. Herskovic A, Martz K, Al-Sarraf M, et al. Combined chemotherapy and radiotherapy compared with radiotherapy alone in patients with cancer of the esophagus. *N Engl J Med*. 1992;326(24):1593-1598.
2. Cooper JS, Guo MD, Herskovic A, et al. Chemoradiotherapy of locally advanced esophageal cancer: long-term follow-up of a prospective randomized trial (RTOG 85–01). Radiation Therapy Oncology Group. *JAMA*. 1999;281(17):1623-1627.
3. Kato K, Muro K, Minashi K, et al. Phase II study of chemoradiotherapy with 5-fluorouracil and cisplatin for Stage II-III esophageal squamous cell carcinoma: JCOG trial (JCOG 9906). *Int J Radiat Oncol Biol Phys*. 2011;81(3):684-690.
4. Minsky BD, Pajak TF, Ginsberg RJ, et al. INT 0123 (Radiation Therapy Oncology Group 94–05) phase III trial of combined-modality therapy for esophageal cancer: high-dose versus standard-dose radiation therapy. *J Clin Oncol*. 2002;20(5):1167-1174.
5. Chang CL, Tsai HC, Lin WC, et al. Dose escalation intensity-modulated radiotherapy-based concurrent chemoradiotherapy is effective for advanced-stage thoracic esophageal squamous cell carcinoma. *Radiother Oncol*. 2017;125(1):73-79.
6. Chen D, Menon H, Verma V, et al. Results of a phase 1/2 trial of chemoradiotherapy with simultaneous integrated boost of radiotherapy dose in unresectable locally advanced esophageal cancer. *JAMA Oncol*. 2019;5(11):1597.
7. Luo HS, Huang HC, Lin LX. Effect of modern high-dose versus standard-dose radiation in definitive concurrent chemoradiotherapy on outcome of esophageal squamous cell cancer: a meta-analysis. *Radiat Oncol*. 2019;14(1):178.
8. Li Y, Zschaeck S, Lin Q, Chen S, Chen L, Wu H. Metabolic parameters of sequential 18F-FDG PET/CT predict overall survival of esophageal cancer patients treated with (chemo-) radiation. *Radiat Oncol*. 2019;14(1):35.
9. Bar-Ad V, Leiby B, Witek M, et al. Treatment-related acute esophagitis for patients with locoregionally advanced non-small cell lung cancer treated with involved-field radiotherapy and concurrent chemotherapy. *Am J Clin Oncol*. 2014;37(5):433-437.
10. Yuan ST, Brown RK, Zhao L, et al. Timing and intensity of changes in FDG uptake with symptomatic esophagitis during radiotherapy or chemo-radiotherapy. *Radiat Oncol*. 2014;9(1):37.

11. Chang S, Koo PJ, Kwak JJ, Kim SJ. Changes in total lesion glycolysis evaluated by repeated F-18 FDG PET/CT as prognostic factor in locally advanced esophageal cancer patients treated with preoperative chemoradiotherapy. *Oncology*. 2016;90(2):97-102.
12. Rebollo Aguirre AC, Ramos-Font C, Villegas Portero R, Cook GJ, Llamas Elvira JM, Tabares AR. 18F-fluorodeoxiglucose positron emission tomography for the evaluation of neoadjuvant therapy response in esophageal cancer: systematic review of the literature. *Ann Surg*. 2009;250(2):247-254.
13. Huang B, Law MW, Khong PL. Whole-body PET/CT scanning: estimation of radiation dose and cancer risk. *Radiology*. 2009;251(1):166-174.
14. Yu CW, Chen XJ, Lin YH, et al. Prognostic value of (18)F-FDG PET/MR imaging biomarkers in oesophageal squamous cell carcinoma. *Eur J Radiol*. 2019;120:108671.
15. Borggreve AS, Goense L, van Rossum PSN, et al. Preoperative prediction of pathologic response to neoadjuvant chemoradiotherapy in patients with esophageal cancer using (18)F-FDG PET/CT and DW-MRI: a prospective multicenter study. *Int J Radiat Oncol Biol Phys*. 2020;106(5):998-1009.
16. van Rossum PS, van Lier AL, van Vulpen M, et al. Diffusion-weighted magnetic resonance imaging for the prediction of pathologic response to neoadjuvant chemoradiotherapy in esophageal cancer. *Radiother Oncol*. 2015;115(2):163-170.
17. Fang P, Musall BC, Son JB, et al. Multimodal imaging of pathologic response to chemoradiation in esophageal cancer. *Int J Radiat Oncol Biol Phys*. 2018;102(4):996-1001.
18. Cao Y, Tsien CI, Nagesh V, et al. Survival prediction in high-grade gliomas by MRI perfusion before and during early stage of RT [corrected]. *Int J Radiat Oncol Biol Phys*. 2006;64(3):876-885.
19. Law M, Young RJ, Babb JS, et al. Gliomas: predicting time to progression or survival with cerebral blood volume measurements at dynamic susceptibility-weighted contrast-enhanced perfusion MR imaging. *Radiology*. 2008;247(2):490-498.
20. Djuric-Stefanovic A, Micev M, Stojanovic-Rundic S, Pesko P, Saranovic D. Absolute CT perfusion parameter values after the neoadjuvant chemoradiotherapy of the squamous cell esophageal carcinoma correlate with the histopathologic tumor regression grade. *Eur J Radiol*. 2015;84(12):2477-2484.
21. Tofts PS, Brix G, Buckley DL, et al. Estimating kinetic parameters from dynamic contrast-enhanced T(1)-weighted MRI of a diffusable tracer: standardized quantities and symbols. *J Magn Reson Imaging*. 1999;10(3):223-232.
22. Landis JR, Koch GG. The measurement of observer agreement for categorical data. *Biometrics*. 1977;33(1):159-174.
23. Yamamoto Y, Kadota T, Yoda Y, et al. Review of early endoscopic findings in patients with local recurrence after definitive chemoradiotherapy for esophageal squamous cell carcinoma. *Esophagus*. 2020;17(4):433-439.
24. Wieder HA, Ott K, Lordick F, et al. Prediction of tumor response by FDG-PET: comparison of the accuracy of single and sequential studies in patients with adenocarcinomas of the esophagogastric junction. *Eur J Nucl Med Mol Imaging*. 2007;34(12):1925-1932.
25. Han S, Kim YJ, Woo S, Suh CH, Lee JJ. Prognostic value of volumetric parameters of pretreatment 18F-FDG PET/CT in esophageal cancer: a systematic review and meta-analysis. *Clin Nucl Med*. 2018;43(12):887-894.
26. Goense L, Borggreve AS, Heethuis SE, et al. Patient perspectives on repeated MRI and PET/CT examinations during neoadjuvant treatment of esophageal cancer. *Br J Radiol*. 2018;91(1086):20170710.
27. Noordman BJ, de Bekker-Grob EW, Coene P, et al. Patients' preferences for treatment after neoadjuvant chemoradiotherapy for oesophageal cancer. *Br J Surg*. 2018;105(12):1630-1638.
28. Hermans R, Meijerink M, Van den Bogaert W, Rijnders A, Weltens C, Lambin P. Tumor perfusion rate determined noninvasively by dynamic computed tomography predicts outcome in head-and-neck cancer after radiotherapy. *Int J Radiat Oncol Biol Phys*. 2003;57(5):1351-1356.
29. Teng F, Aryal M, Lee J, et al. Adaptive boost target definition in high-risk head and neck cancer based on multi-imaging risk biomarkers. *Int J Radiat Oncol Biol Phys*. 2018;102(4):969-977.
30. Hu LS, Eschbacher JM, Heiserman JE, et al. Reevaluating the imaging definition of tumor progression: perfusion MRI quantifies recurrent glioblastoma tumor fraction, pseudoprogression, and radiation necrosis to predict survival. *Neuro Oncol*. 2012;14(7):919-930.
31. Bonekamp D, Deike K, Wiestler B, et al. Association of overall survival in patients with newly diagnosed glioblastoma with contrast-enhanced perfusion MRI: comparison of intraindividually matched T1 - and T2 (*) -based bolus techniques. *J Magn Reson Imaging*. 2015;42(1):87-96.
32. Peerlings J, Van De Voorde L, Mitea C, et al. Hypoxia and hypoxia response-associated molecular markers in esophageal cancer: a systematic review. *Methods*. 2017;130:51-62.
33. Peeters SG, Zegers CM, Yaromina A, Van Elmpt W, Dubois L, Lambin P. Current preclinical and clinical applications of hypoxia PET imaging using 2-nitroimidazoles. *Q J Nucl Med Mol Imaging*. 2015;59(1):39-57.
34. Peeters SG, Zegers CM, Lieuwes NG, et al. A comparative study of the hypoxia PET tracers [(1)(8)F]HX4, [(1)(8)F]FAZA, and [(1)(8)F]FMISO in a preclinical tumor model. *Int J Radiat Oncol Biol Phys*. 2015;91(2):351-359.

SUPPORTING INFORMATION

Additional supporting information may be found in the online version of the article at the publisher's website.

How to cite this article: Wang P, Wang X, Xu L, Yu J, Teng F. Prediction of the effects of radiation therapy in esophageal cancer using diffusion and perfusion MRI. *Cancer Sci*. 2021;112:5046–5054. https://doi.org/10.1111/cas.15156